WCAP-10528

TECHNICAL BASES FOR ELIMINATING LARGE PRIMARY LOOP PIPE RUPTURE AS THE STRUCTURAL DESIGN BASIS FOR COMANCHE PEAK UNITS 1 AND 2

APRIL, 1984

Prepared By: S. A. Swamy
E. L. Furchi
H. F. CLark, Jr.
A. D. Sane
W. H. Bamford

APPROVED: _____
J. N. Chirigos, Mgr.
Structural Materials
Engineering

APPROVED: _____
E. R. Johnson, Mgr.
Structural and Seismic
Development

APPROVED: _____
J. J. McInerney, Mgr.
Mechanical Equipment
and Systems Licensing

WESTINGHOUSE ELECTRIC CORPORATION
NUCLEAR ENERGY SYSTEMS
P.O. BOX 355
PITTSBURGH, PENNSYLVANIA 15230

TABLE OF CONTENTS

LIST OF TABLES

LIST OF FIGURES

1.0 INTRODUCTION

1.1 Purpose

This report applies to the Comanche Peak plant reactor coolant system primary loop piping. It is intended to demonstrate that specific parameters for the Comanche Peak plant are enveloped by the generic analysis performed by Westinghouse in WCAP-9558, Revision 2 (Reference 1) and accepted by the NRC (Reference 4).

1.2 Scope

The current structural design basis for the Reactor Coolant System (RCS) primary loop requires that pipe breaks be postulated as defined in the approved Westinghouse Topical Report WCAP-8082 (Reference 5). In addition, protective measures for the dynamic effects associated with RCS primary loop pipe breaks have been incorporated in the Comanche Peak plant design. However, Westinghouse has demonstrated on a generic basis that RCS primary loop pipe breaks are highly unlikely and should not be included in the structural design basis of Westinghouse plants (see Reference 6). In order to demonstrate this applicability of the generic evaluations to the Comanche Peak plant, Westinghouse has performed: a comparison of the loads and geometry for the Comanche Peak plant with envelope parameters used in the generic analyses (Reference 1), a fracture mechanics evaluation, a determination of leak rates from a through-wall crack, fatigue crack growth evaluation, and an assessment of margins.

1.3 Objectives

The conclusions of WCAP-9558, Revision 2[1] support the elimination of RCS primary loop pipe breaks for the Comanche Peak plant. In order to validate this conclusion the following objectives must be achieved.

a. Demonstrate that Comanche Peak plant parameters are enveloped by generic Westinghouse studies.

b. Demonstrate that margin exists between the critical crack size and a postulated crack which yields a detectable leak rate.

c. Demonstrate that there is sufficient margin between the leakage through a postulated crack and the leak detection capability of the Comanche Peak plant.

d. Demonstrate that fatigue crack growth is negligible.

1.4 Background Information

Westinghouse has performed considerable testing and analysis to demonstrate that RCS primary loop pipe breaks can be eliminated from the structural design basis of all Westinghouse plants. The concept of eliminating pipe breaks in the RCS primary loop was first presented to the NRC in 1978 in WCAP-9283 (Reference 7). This Topical Report employed a deterministic fracture mechanics evaluation and a probabilistic analysis to support the elimination of RCS primary loop pipe breaks.

This approach was then used as a means of addressing Generic Issue A-2 and Asymmetric LOCA Loads. Westinghouse performed additional testing and analysis to justify the elimination of RCS primary loop pipe breaks. As a result of this effort, WCAP-9558, Revision 2, WCAP-9787, and Letter Report NS-EPR-2519 (References 1, 2, and 3) were submitted to the NRC.

The NRC funded research through Lawrence Livermore National Laboratory (LLNL) to address this same issue using a probabilistic approach. As part of the LLNL research effort, Westinghouse performed extensive evaluations of specific plant loads, material properties, transients, and system geometries to demonstrate that the analysis and testing previously performed by Westinghouse and the research performed by LLNL applied to all Westinghouse plants including Comanche Peak (References 8 and 9). The results from the LLNL study

were released at a March 28, 1983 ACRS Subcommittee meeting. These studies which are applicable to all Westinghouse plants east of the Rocky Mountains, determined the mean probability of a direct LOCA (RCS primary loop pipe break) to be 10^{-10} per reactor year and the mean probability of an indirect LOCA to be 10^{-7} per reactor year. Thus, the results previously obtained by Westinghouse (Reference 7) were confirmed by an independent NRC research study.

Based on the studies by Westinghouse, by LLNL, the ACRS, and the AIF, the NRC completed a safety review of the Westinghouse reports submitted to address asymmetric blowdown loads that result from a number of discrete break locations on the PWR primary systems. The NRC Staff evaluation[4] concludes that an acceptable technical basis has been provided so that asymmetric blowdown loads need not be considered for those plants that can demonstrate the applicability of the modeling and conclusions contained in the Westinghouse response or can provide an equivalent fracture mechanics demonstration of the primary main coolant loop integrity.

This report will demonstrate the applicability of the Westinghouse generic evaluations to the Comanche Peak plant.

2.0 OPERATION AND STABILITY OF THE REACTOR COOLANT SYSTEM

The Westinghouse reactor coolant system primary loop has an operating history which demonstrates its inherent stability characteristics of the design. This includes a low susceptibility to cracking failure from the effects of corrosion (e.g., intergranular stress corrosion cracking), water hammer, or fatigue (low and high cycle). This operating history totals over 400 reactor-years, including five plants each having 15 years of operation and 15 other plants each with over 10 years of operation.

2.1 Stress Corrosion Cracking

For the Westinghouse plants, there is no history of cracking failure in the reactor coolant system loop piping. For stress corrosion cracking (SCC) to occur in piping, the following three conditions must exist simultaneously: high tensile stresses, a susceptible material, and a corrosive environment (Reference 10). Since some residual stresses and some degree of material susceptibility exist in any stainless steel piping, the potential for stress corrosion is minimized by proper material selection immune to SCC as well as preventing the occurrence of a corrosive environment. The material specifications consider compatibility with the system's operating environment (both internal and external) as well as other materials in the system, applicable ASME Code rules, fracture toughness, welding, fabrication, and processing.

The environments known to increase the susceptibilty of austenitic stainless steel to stress corrosion are (Reference 10): oxygen, fluorides, chlorides, hydroxides, hydrogen peroxide, and reduced forms of sulfur (e.g., sulfides, sulfites, and thionates). Strict pipe cleaning standards prior to operation and careful control of water chemistry during plant operation are used to prevent the occurrence of a corrosive environment. Prior to being put into service, the piping is cleaned internally and externally. During flushes and preoperational testing, water chemistry is controlled in accordance with written specifications. External cleaning for Class 1 stainless steel piping includes patch tests to monitor and control chloride and fluoride levels. For preoperational flushes, influent water chemistry is controlled. Requirements on chlorides, fluorides, conductivity, and pH are included in the acceptance criteria for the piping.

During plant operation, the reactor coolant water chemistry is monitored and maintained within very specific limits. Contaminant concentrations are kept below the thresholds known to be conducive to stress corrosion cracking with the major water chemistry control standards being included in the plant operating procedures as a condition for plant operation. For example, during normal power operation, oxygen concentration in the RCS is expected to be less than 0.005 ppm by controlling charging flow chemistry and maintaining hydrogen in the reactor coolant at specified concentrations. Halogen concentrations are also stringently controlled by maintaining concentrations of chlorides and fluorides within the specified limits. This is assured by controlling charging flow chemistry and specifying proper wetted surface materials.

2.2 Water Hammer

Overall, there is a low potential for water hammer in the RCS since it is designed and operated to preclude the voiding condition in normally filled lines. The reactor coolant system, including piping and primary components, is designed for normal, upset, emergency, and faulted condition transients. The design requirements are conservative relative to both the number of transients and their severity. Relief valve actuation and the associated hydraulic transients following valve opening are considered in the system design. Other valve and pump actuations are relatively slow transients with no significant effect on the system dynamic loads. To ensure dynamic system stability, reactor coolant parameters are stringently controlled. Temperature during normal operation is maintained within a narrow range by control rod position; pressure is controlled by pressurizer heaters and pressurizer spray also within a narrow range for steady-state conditions. The flow characteristics of the system remain constant during a fuel cycle because the only governing parameters, namely system resistance and the reactor coolant pump characteristics are controlled in the design process. Additionally, Westinghouse has instrumented typical reactor coolant systems to verify the flow and vibration characteristics of the system. Preoperational testing and operating experience have verified the Westinghouse approach. The operating transients of the RCS primary piping are such that no significant water hammer can occur.

2.3 Low Cycle and High Cycle Fatigue

Low cycle fatigue considerations are accounted for in the design of the piping system through the fatigue usage factor evaluation to show compliance with the rules of Section III of the ASME Code. A further evaluation of the low cycle fatigue loadings was carried out as part of this study in the form of a fatigue crack growth analysis, as discussed in Section 6.

High cycle fatigue loads in the system would result primarily from pump vibrations. These are minimized by restrictions placed on shaft vibrations during hot functional testing and operation. During operation, an alarm signals the exceedance of the vibration limits. Field measurements have been made on a number of plants during hot functional testing, including plants similar to Comanche Peak. Stresses in the elbow below the RC pump have been found to be very small, between 2 and 3 ksi at the highest. These stresses are well below the fatigue endurance limit for the material, and would also result in an applied stress intensity factor below the threshold for fatigue crack growth.

3.0 PIPE GEOMETRY AND LOADING

A segment of the primary coolant hot leg pipe is shown in Figure 1. This segment is postulated to contain a circumferential through-wall flaw. The inside diameter and wall thickness of the pipe are 29.0 and 2.45 inches, respectively. The pipe is subjected to a normal operating pressure of [ ]^{a,c,e} psi. Figure 2 identifies the loop weld locations. The material properties and the loads at these locations resulting from deadweight, thermal expansion and Safe Shutdown Earthquake are indicated in Table 1. As seen from this Table, the junction of hot leg and the reactor vessel outlet nozzle is the worst location for crack stability analysis based on the highest stress due to combined pressure, dead weight, thermal expansion, and SSE (Safe Shutdown Earthquake) loading. At this location, the axial load (F) and the bending moment (M) are [ ]^{a,c,e} (including axial force due to pressure) and [ ]^{a,c,e}, respectively. The loads of Table 1 are calculated as follows:

The axial force F and transverse bending moments, M_y and M_z, are chosen for each static load (pressure, deadweight and thermal) based on elastic-static analyses for each of these load cases. These pipe load components are combined algebraically to define the equivalent pipe static loads F_s, M_{ys}, and M_{zs}. Based on elastic SSE response spectra analyses, amplified pipe seismic loads, F_d, M_{yd}, M_{zd} are obtained. The maximum pipe loads are obtained by combining the static and dynamic load components as follows:

$$F = |F_s| + |F_d|$$

$$M = \sqrt{M_y^2 + M_z^2}$$

where:

$$M_y = |M_{ys}| + |M_{yd}|$$

$$M_z = |M_{zs}| + |M_{zd}|$$

The corresponding geometry and loads used in the reference report (Reference 1) are as follows: inside diameter and wall thickness are 29.0 and 2.5 inches; axial load and bending moment are [ ]^{a,c,e} inch-kips. The outer fiber stress for Comanche Peak is [ ]^{a,c,e} ksi, while for the reference report it is [ ]^{a,c,e} ksi. This demonstrates conservatism in the reference report which makes it more severe than the Comanche Peak project.

The normal operating loads (i.e., algebric sum of pressure, deadweight, and 100 percent power thermal expansion loading) at the critical location, i.e., the junction of hot leg and the reactor vessel outlet nozzle are as follows:

F = [ ]^{a,c,e} (including internal pressure)
M = [ ]^{a,c,e}

The calculated and allowable stresses for ASME equation 9 (faulted) and equation 12 at the critical location are as follows:

Equation Number	Calculated Stress (ksi)	Allowable Stress (ksi)	Ratio of Calculated/ Allowable
[			] a,c,e

4.0 FRACTURE MECHANICS EVALUATION

4.1 Global Failure Mechanism

Determination of the conditions which lead to failure in stainless steel must be done with plastic fracture methodology because of the large amount of deformation accompanying fracture. A conservative method for predicting the failure of ductile material is the [

]^{a,c,e} This methodology has been shown to be applicable to ductile piping through a large number of experiments, and will be used here to predict the critical flaw size in the primary coolant piping. The failure criterion has been obtained by requiring [

]^{a,c,e} (Figure 3) when loads are applied. The detailed development is provided in Appendix A, for a through-wall circumferential flaw in a pipe with internal pressure, axial force, and imposed bending moments. The [

]^{a,c,e} for such a pipe is given by:

[ ] a,c,e

where:

[ ] a,c,e

[ ]a,c,e

The analytical model described above accurately accounts for the piping internal pressure as well as imposed axial force as they affect [ ]a,c,e Good agreement was found between the analytical predictions and the experimental results [11].

4.2 Local Failure Mechanism

The local mechanism of failure is primarily dominated by the crack tip behavior in terms of crack-tip blunting, initiation, extension and finally crack instability. Depending on the material properties and geometry of the pipe, flaw size, shape and loading, the local failure mechanisms may or may not govern the ultimate failure.

The stability will be assumed if the crack does not initiate at all. It has been accepted that the initiation toughness, measured in terms of J_{IN} from a J-integral resistance curve is a material parameter defining the crack initiation. If, for a given load, the calculated J-integral value is shown to be less than J_{IN} of the material, then the crack will not initiate. If the initiation criterion is not met, one can calculate the tearing modulus as defined by the following relation:

$$T_{app} = \frac{dJ}{da} \quad \frac{E}{\sigma_f^2}$$

where:

T_{app} = applied tearing modulus

E = modulus of elasticity

σ_f = [ ]^{a,c,e} (flow stress)

a = crack length

[ ]^{a,c,e}

In summary, the local crack stability will be established by the two-step criteria:

$$J < J_{IN}$$

$$T_{app} < T_{mat} \quad \text{if } J > J_{IN}$$

4.3 Material Properties

The materials in the Comanche Peak Units 1 and 2 primary loops are cast stainless steel (SA 351 CF8A) and associated welds. The tensile and flow properties of the limiting location, the hot leg and reactor outlet nozzle junction, are given in Figure 5, which will be discussed further in the next section.

The fracture properties of CF8A cast stainless steel have been determined through fracture tests carried out at 600°F and reported in Reference 12. This reference shows that J_{IN} for the base metal ranges from [ ]^{a,c,e} for the multiple tests carried out.

Cast stainless steels are subject to thermal aging during service. This thermal aging causes an elevation in the yield strength of the material and a degradation of the fracture toughness, the degree of degradation being proportional to the level of ferrite in the material. To determine the effects of thermal aging on piping integrity a detailed study was carried out in Reference 16. In this report, fracture toughness results were presented for a material representative of [ ]^{a,c,e} Toughness results were provided for the material in the fully aged condition and these properties are also presented in Figure 4 of this report for information. The J_{IN} value for this material at operating

temperature was approximately [ ]^{a,c,e} and the maximum value of J obtained in the tests was in excess of [ ]^{a,c,e} The tests of this material were conducted on small specimens and therefore rather short crack extensions, (maximum extension 4.3 mm) so it is expected that much higher J values would be sustained for larger specimens. The effect of the aging process on loop piping integrity for Comanche Peak was addressed in Reference 16, where the plant specific material chemistry for all the loop materials was considered [ ].^{a,c,e} This reference shows that the degree of thermal aging expected by end-of-life for these units is much less than that which was produced in [ ]^{a,c,e} and therefore the J_{IN} values for the Comanche Peak Units 1 and 2 after end-of-life would be expected to be much higher than those reported for [ ]^{a,c,e} in Figure 4[18]. In addition, the tearing modulus for the Comanche Peak Units 1 and 2 materials would be greater than [ ]^{a,c,e}

Available data on stainless steel welds indicate the J_{IN} values for the worst case welds are of the same order as the aged material, but the slope of the J-R curve is steeper, and higher J-values have been obtained from fracture tests (in excess of 3000 in-lb/in^2). The applied value of J integral for a flaw in the weld regions will be lower than that in the base metal because the yield stress for the weld materials is much higher at temperature. Therefore, weld regions are less limiting than the cast material.

4.4 Results of Crack Stability Evaluation

Figure 5 shows a plot of the [ ]^{a,c,e} as a function of through-wall circumferential flaw length in the [ ]^{a,c,e} of the main coolant piping. This [ ]^{a,c,e} was calculated for Comanche Peak data of a pressurized pipe at [ ]^{a,c,e} properties. The maximum applied bending moment of [ ]^{a,c,e} in-kips can be plotted on this figure, and used to determine the critical flaw length, which is shown to be [ ]^{a,c,e} inches. This is considerably larger than the [ ]^{a,c,e} inch reference flaw used in Reference 1.

[

]^{a,c,e} Therefore, it can be concluded that a postulated [ ]^{a,c,e} inch through-wall flaw in the Comanche Peak loop piping will remain stable from both a local and global stability standpoint.

A finite element elastic-plastic analysis was performed for a [ ]^{a,c,e} through-wall flaw using the same approach and material properties described in detail in Reference 1. The purpose of this calculation was to investigate the crack stability for a postulated flaw larger in size than the [ ]^{a,c,e} reference flaw. For the Comanche Peak Units 1 and 2 maximum load of [ ]^{a,c,e} the maximum applied J was calculated to be [ ]^{a,c,e} Therefore, it is further concluded that a postulated [ ]^{a,c,e} through-wall flaw in the Comanche Peak Units 1 and 2 primary loop piping will remain stable from both a local and global stability standpoint. Accordingly, the "critical" flaw size will be even greater than [ ]^{a,c,e}

5.0 LEAK RATE PREDICTIONS

Leak rate calculations were performed in Reference 1 using an initial through-wall crack [ ]^{a,c,e}. The computed leak rate was [ ]^{a,c,e} based on the normal operating pressure of [ ]^{a,c,e} psi. [ ]^{a,c,e} piping under present investigation are very similar, a leak rate of 10 gpm would be reached when the pipe is subjected to the normal operating pressure [ ]^{a,c,e} This computed leak rate [ ]^{a,c,e} significantly exceeds the smallest detectable leak rate for the plant. The Comanche Peak plant has a RCS pressure boundary leak detection system which is consistent with the guidelines of Regulatory Guide 1.45 and can detect leakage of 1 gpm in one hour. There is a factor of [ ]^{a,c,e} between the calculated leak rate and the Comanche Peak plant leak detection systems.

Leak rate estimates were refined by applying the normal operating bending moment of [ ]^{a,c,e} in addition to the normal operating pressure of [ ]^{a,c,e} These loads were applied to the hot leg pipe containing a postulated [ ]^{a,c,e} through-wall flaw and the crack opening area was estimated using the method of Reference 17. The leak rate was calculated using the two-phase flow formulation described in Reference 1. The computed leak rate was significantly greater than [ ]^{a,c,e} In order to determine the sensitivity of leak rate to flaw size, a through-wall flaw [ ]^{a,c,e} in length was postulated. The calculated leak rate was greater [ ]^{a,c,e}

Thus, there is a factor of at least [ ]^{a,c,e} between the calculated leak rate for a [ ]^{a,c,e} flaw and the Regulatory Guide 1.45 leak detection criteria.

6.0 FATIGUE CRACK GROWTH ANALYSIS

To determine the sensitivity of the primary coolant system to the presence of small cracks, a fatigue crack growth analysis was carried out for the [ ]^{a,c,e} region of a typical system. This region was selected because it is typically one of the highest stressed cross sections, and crack growth calculated here will be conservative for application to the entire primary coolant system.

A finite element stress analysis was carried out for the [ ]^{a,c,e} of a plant typical in geometry and operational characteristics to any Westinghouse PWR System. [

]^{a,c,e}

All normal, upset, and test conditions were considered and circumferentially oriented surface flaws were postulated in the region, assuming the flaw was located in three different locations, as shown in Figure 6. Specifically, these were:

Cross Section A: [
Cross Section B:
Cross Section C:] a,c,e

Fatigue crack growth rate laws were used [

]^{a,c,e} The law for stainless steel was derived from Reference 13, with a very conservative correction for R ratio, which is the ratio of minimum to maximum stress during a transient.

$$\frac{da}{dn} = (5.4 \times 10^{-12}) K_{eff}^{4.48} \text{ inches/cycle}$$

where $K_{eff} = K_{max} (1-R)^{0.5}$

$R = K_{min}/K_{max}$

[

]a,c,e

[ ]a,c,e

where: [ ]a,c,e

The calculated fatigue crack growth for semi-elliptic surface flaws of circumferential orientation and various depths is summarized in Table 2, and shows that the crack growth is very small, regardless [

]a,c,e

7.0 ASSESSMENT OF MARGINS

In Reference 1, the maximum design load was [ ]^{a,c,e} in-kips, whereas, the maximum load as noted in Section 3.0 of this report is significantly less, [ ]^{a,c,e} in-kips. For the current application, the maximum value of J [ ]^{a,c,e} in-lb/in^2 compared with the value of [ ]^{a,c,e} in-lb/in^2 in Reference 1. Furthermore, Section 4.3 shows that the testing of fully aged material of chemistry worse than that existing in Comanche Peak cast piping extended to J values of [ ]^{a,c,e} in-lb/in^2; this is greater than the maximum value of applied J of [ ]^{a,c,e} in-lb/in^2. At maximum load the Comanche Peak Units 1 and 2 applied J-value is enveloped by the J_{max} of Reference 1 as well as the values used in testing fully aged material.

In Section 4.4, it is seen that a [ ]^{a,c,e} flaw has a J value at maximum load of [ ] in-lb/in^2 which is also enveloped by the J_{max} of Reference 1 and the value used for testing of aged material. In Section 4.4, the "critical" flaw size using [ ]^{a,c,e} methods is calculated to be [ ]^{a,c,e} inches. Based on the above, the "critical" flaw size will, of course, exceed [ ]^{a,c,e}

Again, referring to Section 4.3, the estimated tearing modulus for Comanche Peak Units 1 and 2 cast SS piping in the fully aged condition is at least [ ].^{a,c,e} $T_{applied}$ as taken from Reference 16 is [ ]^{a,c,e} Consequently, a margin on local stability of at least [ ]^{a,c,e} exists relative to tearing.

In Section 5.0, it is shown that a flaw of less than [ ]^{a,c,e} would yield a leak rate of [ ]^{a,c,e} Thus, there is a factor of at least [ ]^{a,c,e} between the minimum flaw size that gives a leak rate of [ ]^{a,c,e} and the "critical" flaw size of [ ]^{a,c,e}

In summary, relative to

1. Loads

   Comanche Peak Unit 1 and 2 are enveloped both by the maximum loads and J values in Reference 1 and the J values employed in testing of fully aged material.

2. Flaw Size

   a. A margin of at least [ ]^{a,c,e} exists between the "critical" flaw and the flaw yielding a leak rate of [ ]^{a,c,e}

   b. A margin exists of at least [ ]^{a,c,e} relative to tearing.

   c. A margin exists of at least [ ]^{a,c,e} relative to global stability. If [ ]^{a,c,e} is used as the basis for "critical" flaw size, the margin for global stability would be at least [ ]^{a,c,e}

3. Leak Rate

   A margin of at least [ ]^{a,c,e} exists between calculated leak rates and the criteria of Regulatory Guide 1.45.

8.0 CONCLUSIONS

This report has established the applicability of the generic Westinghouse evaluations which justify the elimination of RCS primary loop pipe breaks for the Comanche Peak plant as follows:

a. The loads, material properties, transients, and geometry relative to the Comanche Peak Units 1 and 2 RCS primary loop are enveloped by the parameters of WCAP-9558, Revision 2[1] and WCAP-10456.[16]

b. Stress corrosion cracking is precluded by use of fracture resistant materials in the piping system and controls on reactor coolant chemistry, temperature, pressure, and flow during normal operation.

c. Water hammer should not occur in the RCS piping because of system design, testing, and operational considerations.

d. The effects of low and high cycle fatigue on the integrity of the primary piping are negligible.

e. Ample margin exists between the leak rate of the reference flaw and the criteria of Reg. Guide 1.45.

f. Ample margin exists between the reference flaw chosen for leak detectability and the "critical" flaw.

g. Ample margin exists in the material properties used to demonstrate end-of-life (relative to aging) stability of the reference flaw.

The reference flaw will be stable throughout reactor life because of the ample margins in e, f, and g, above, and will leak at a detectable rate which will assure a safe plant shutdown.

Based on the above, it is concluded that RCS primary loop pipe breaks should not be considered in the structural design basis of the Comanche Peak plant.

9.0 PEFERENCES

1. WCAP-9558, Rev. 2, "Mechanistic Fracture Evaluation of Reactor Coolant Pipe Containing a Postulated Circumferential Through-Wall Crack," Westinghouse Proprietary Class 2, June 1981.

2. WCAP-9787, "Tensile and Toughness Properties of Primary Piping Weld Metal for Use in Mechanistic Fracture Evaluation", Westinghouse Proprietary Class 2, May 1981.

3. Letter Report NS-EPR-2519, Westinghouse (E. P. Rahe) to NRC (D. G. Eisenhut), Westinghouse Proprietary Class 2, November 10, 1981.

4. USNRC Generic letter 84-04, Subject: "Safety Evaluation of Westinghouse Topical Reports Dealing with Elimination of Postulated Pipe Breaks in PWR Primary Main Loops", February 1, 1984.

5. WCAP-8082 P-A, "Pipe Breaks for the LOCA Analysis of the Westinghouse Primary Coolant Loop," Class 2, January 1975.

6. Letter from Westinghouse (E. P. Rahe) to NRC (R. H. Vollmer), NS-EPR-2768, dated May 11, 1983.

7. WCAP-9283, "The Integrity of Primary Piping Systems of Westinghouse Nuclear Power Plants During Postulated Seismic Events," Westinghouse Proprietary Class 2, March, 1978.

8. Letter from Westinghouse (E. P. Rahe) to NRC (W. V. Johnson) dated April 25, 1983.

9. Letter from Westinghouse (E. P. Rahe) to NRC (W. V. Johnston) dated July 25, 1983.

10. NUREG-0691, "Investigation and Evaluation of Cracking Incidents in Piping in Pressurized Water Reactors", USNRC, September 1980.

11. Kanninen, M. F., et. al., "Mechanical Fracture Predictions for Sensitized Stainless Steel Piping with Circumferential Cracks", EPRI NP-192, September 1976.

12. Bush, A. J., Stoofer, R. B., "Fracture Toughness of Cast 316 SS Piping Material Heat No. 156576, at 600°F", W R D Memo No. 83-5P6EVMTL-M1, Westinghouse Proprietary Class 2, March 7, 1983.

13. Bamford, W. H., "Fatigue Crack Growth of Stainless Steel Piping in a Pressurized Water Reactor Environment", Trans. ASME Journal of Pressure Vessel Technology, Vol. 101, Feb. 1979.

14. [ ] a,c,e

15. [ ] a,c,e

16. WCAP-10456, "The Effects of Thermal Aging on the Structural Integrity of Cast Stainless Steel Piping For W NSSS," W Proprietary Class 2, November 1983.

17. NUREG/CR-3464, 1983, "The Application of Fracture Proof Design Methods using Tearing Instability Theory to Nuclear Piping Postulating Circumferential Through Wall Cracks"

18. Slama, G., Petrequin, P., Masson, S. H., and Mager, T. R., "Effect of Aging on Mechanical Properties of Austenitic Stainless Steel Casting and Welds", presented at SMiRT 7 Post Conference Seminar 6 - Assuring Structural Integrity of Steel Reactor Pressure Boundary Components, August 29/30, 1983, Monterey, CA.

TABLE 1

COMANCHE PEAK PRIMARY LOOP DATA

[a,c,e]

TABLE 2

FATIGUE CRACK GROWTH AT [ ]a,c,e (40 YEARS)

	FINAL FLAW (in)		
INITIAL FLAW (IN)	[ ]a,c,e	[ ]a,c,e	[ ]a,c,e
0.292	0.31097	0.30107	0.30698
0.300	0.31949	0.30953	0.31626
0.375	0.39940	0.38948	0.40763
0.425	0.45271	0.4435	0.47421

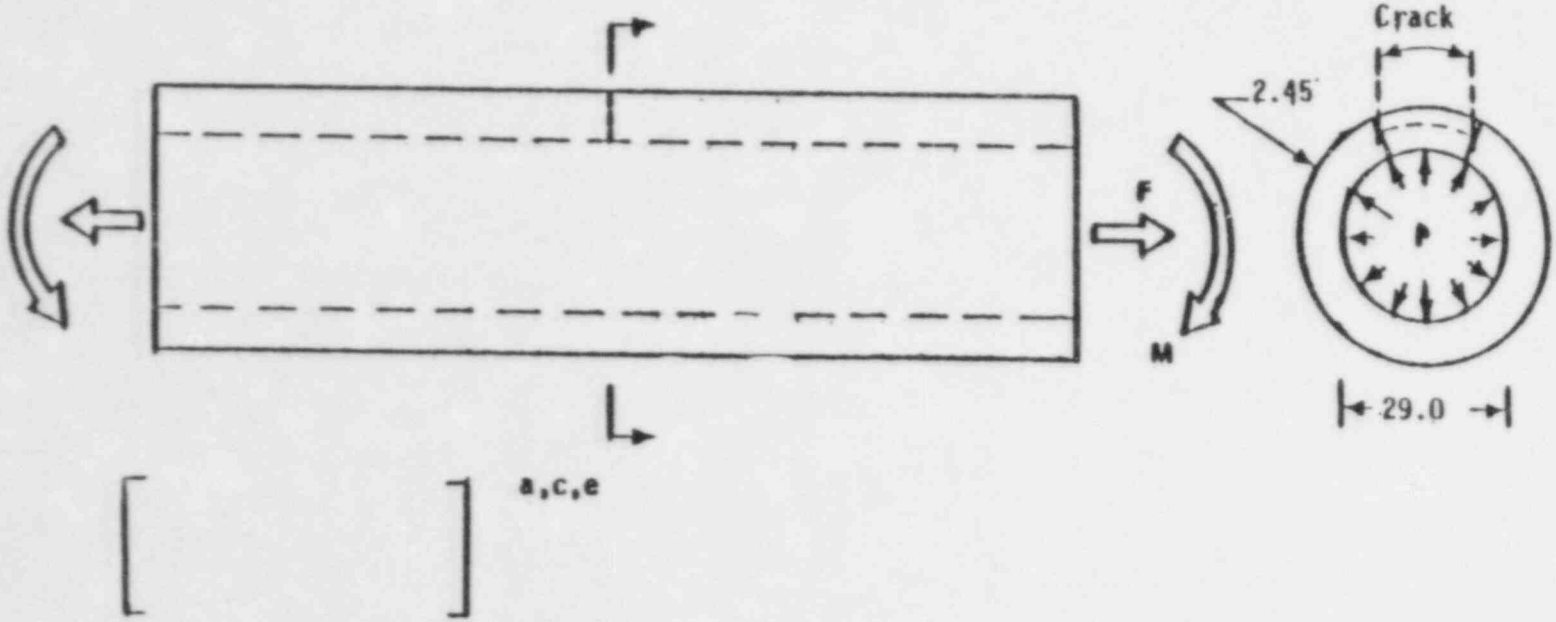

FIGURE 1 REACTOR COOLANT PIPE

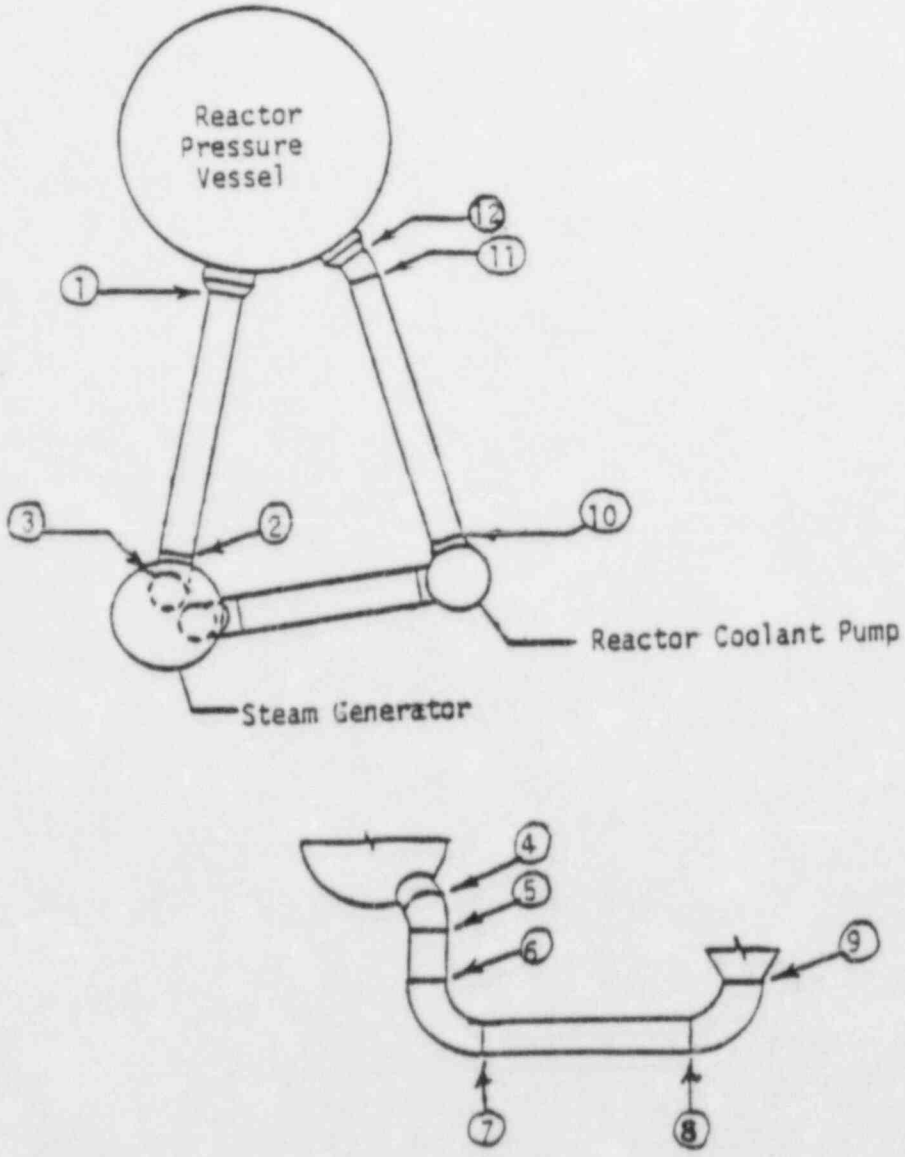

[ ] a,c,e

FIGURE 2 SCHEMATIC DIAGRAM OF PRIMARY LOOP SHOWING WELD LOCATIONS

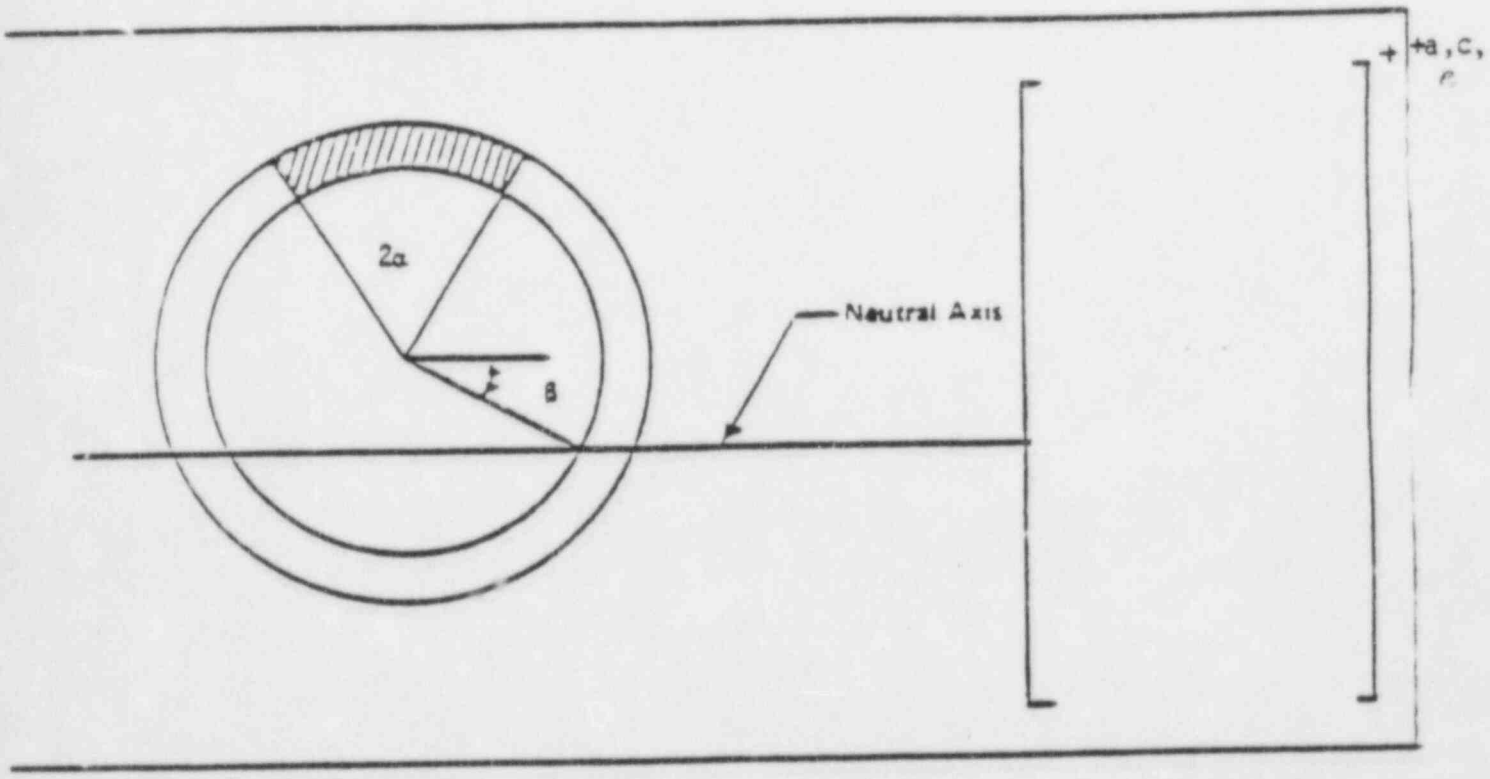

FIGURE 3 [ ] STRESS DISTRIBUTION

a,c,e

J, K J/m²

FIGURE 4 J-Δa CURVES AT DIFFERENT TEMPERATURES. AGED MATERIAL [ ]a,c,e
(7500 HOURS AT 400°C)

a,c,e

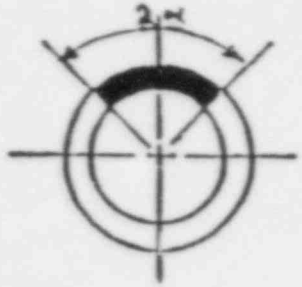

FLAW GEOMETRY

FIGURE 5 CRITICAL FLAW SIZE PREDICTION

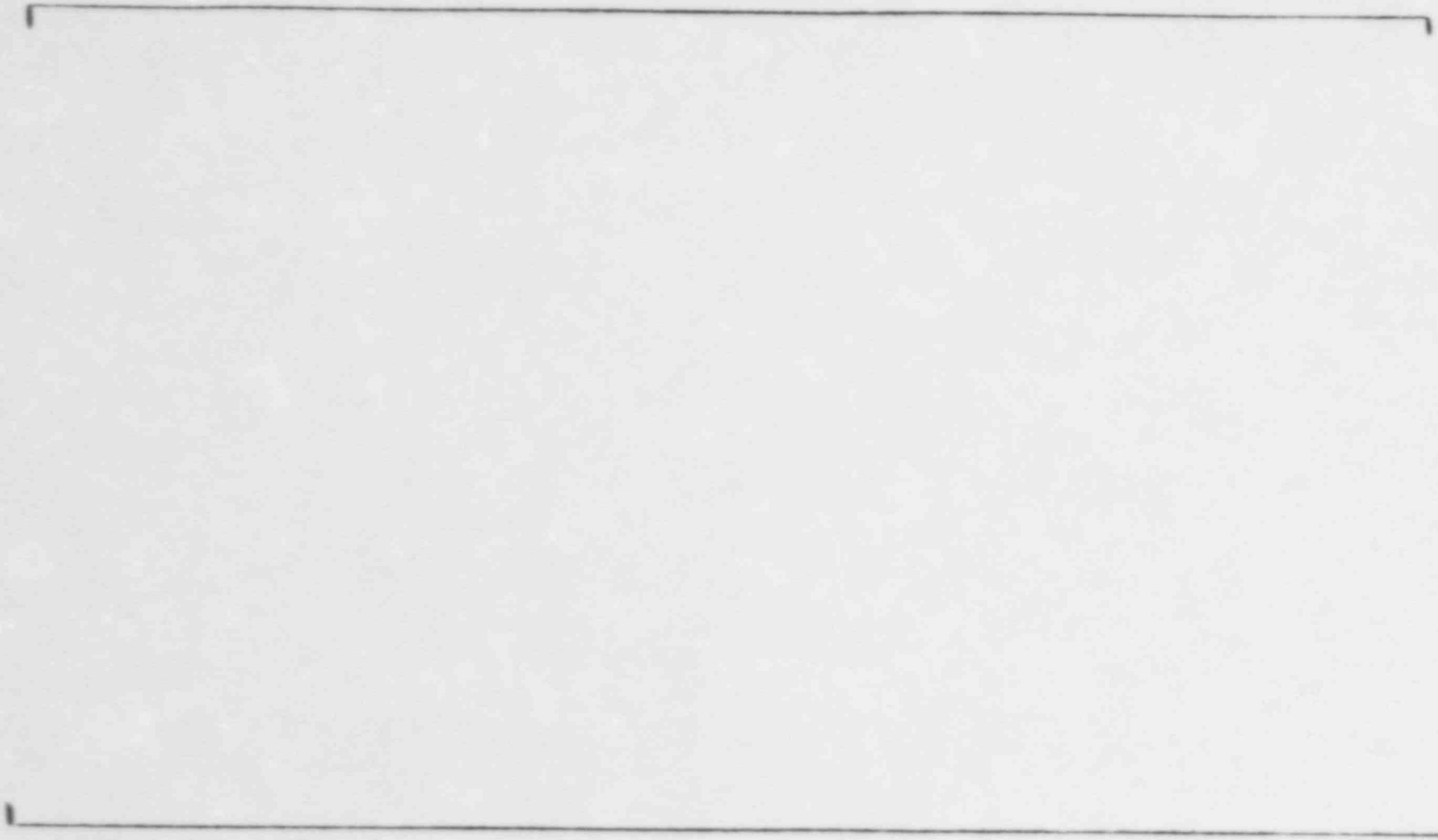

FIGURE 6 TYPICAL CROSS-SECTION OF [ ] a,c,e

a,c,e

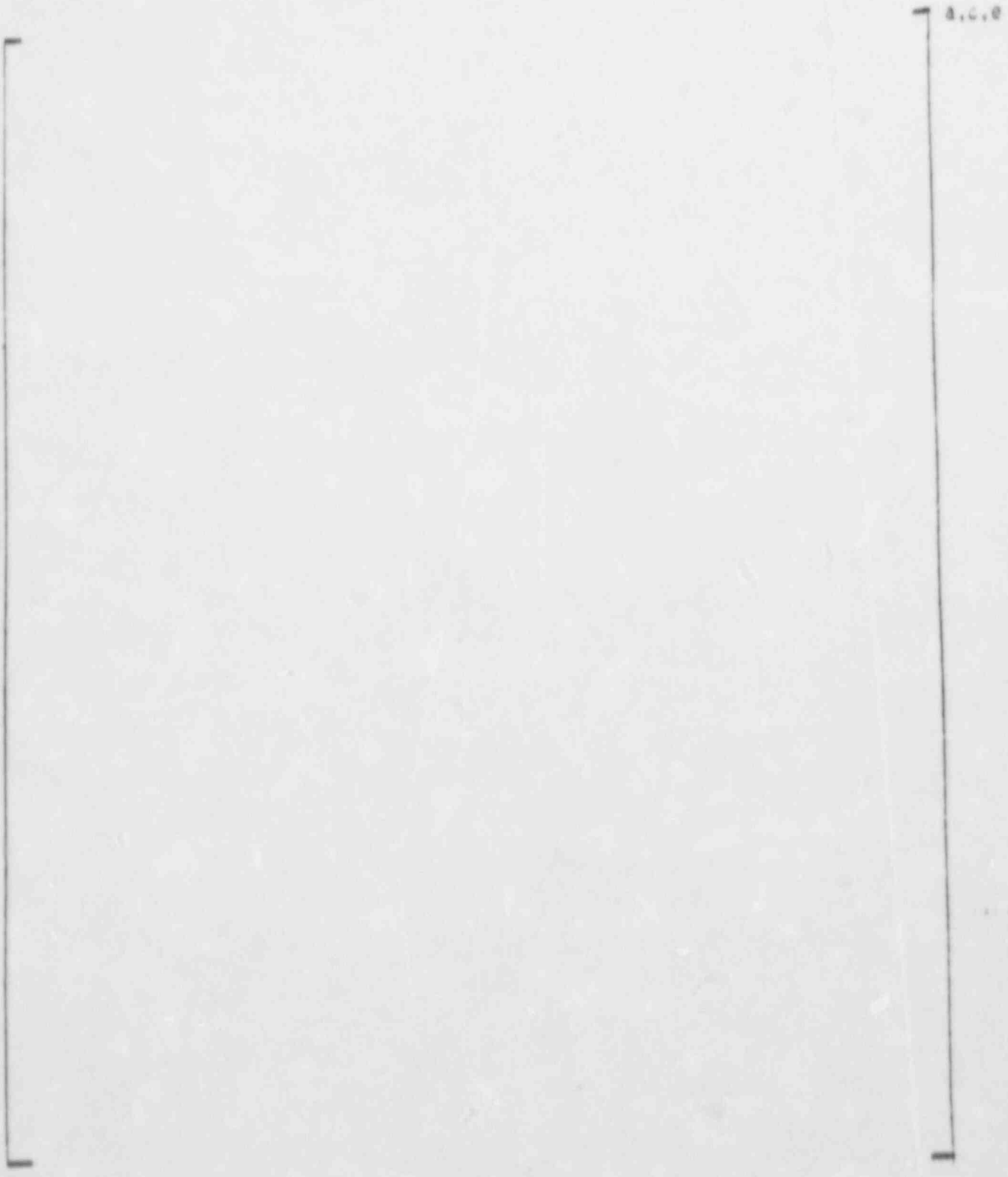

FIGURE 7 REFERENCE FATIGUE CRACK GROWTH CURVES FOR [ ] a,c,e

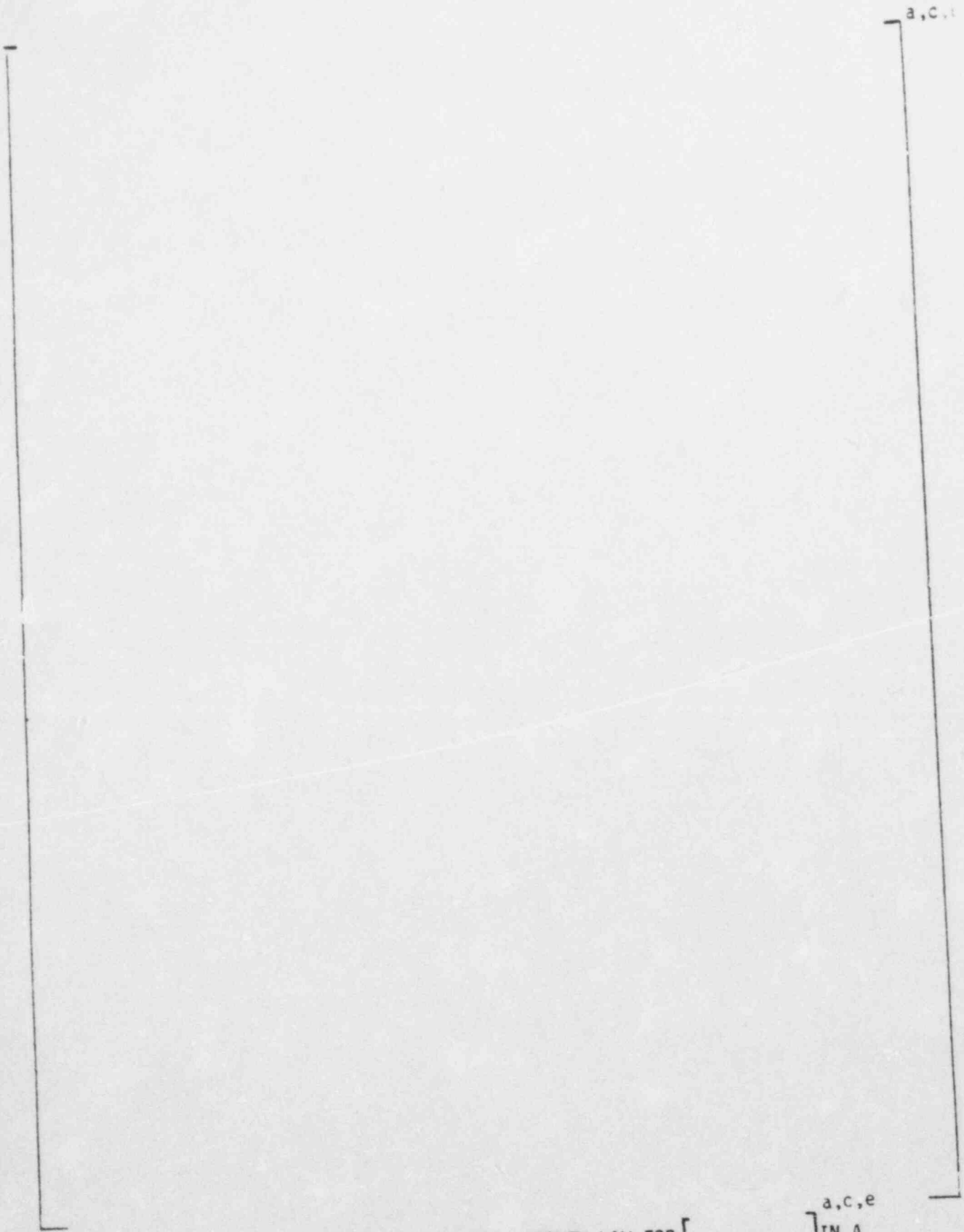

FIGURE 8 REFERENCE FATIGUE CRACK GROWTH LAW FOR [a,c,e] IN A WATER ENVIRONMENT AT 600F

APPENDIX A

[a,c,e]

[a,c,e]

FIGURE A-1 PIPE WITH A THROUGH-WALL CRACK IN BENDING